Predicting ε_{50} for Lateral Response of Piles in Marine Clay Using an Evolutionary-Based Approach

Babak Ebrahimian [1], Aida Nazari [2]

[1] Department of Infrastructure & Offshore Geotechnics (DIOG), Petroleum Industry Research Engineering Company (PIRE Co.), Tehran, Iran; ebrahimian.babak@gmail.com, ebrahimian@pireco.ir
[2] Department of Infrastructure & Offshore Geotechnics (DIOG), Petroleum Industry Research Engineering Company (PIRE Co.), Tehran, Iran; nazari.aida@gmail.com, nazari.a@pireco.ir

Abstract
Analyzing piles subjected to lateral loads significantly depends on soil resistance at any point along the pile as a function of pile deflection, known as p-y curve. On the other hand, the deformation characteristics of soil defined as "the soil strain at 50% of maximum deviatoric stress (ε_{50})" has considerable effect on the generated p-y curve. In this research, several models are proposed to predict ε_{50} specifically for designing very long pile foundations of offshore oil and gas platforms in South Pars field, Persian Gulf, Iran. Herein, ε_{50} is evaluated from extensive soil data of marine clays including in-situ and laboratory test results using evolutionary polynomial regression (EPR). It is demonstrated that the normalized cone tip resistance, which is an indication of soil undrained shear strength, leads to more realistic ε_{50} values compared with the laboratory-derived undrained shear strength parameter. Furthermore, the results of a numerical study on lateral pile-soil system are used in order to show the efficiency of the proposed model in predicting lateral pile response.

Keywords: p-y curve, laterally loaded pile, piezocone penetration test (PCPT), marine clay, evolutionary polynomial regression (EPR), South Pars field

Introduction

Pile foundations are often required to be designed against significant lateral in addition to vertical loads. These lateral loads can be imposed by wind, earth pressure, wave, tide, current and ship impact, mooring rope, earthquake, vehicle traction and etc. The performance of pile foundations is usually governed by either deflection or bearing capacity. Exceeding the maximum allowable lateral load may cause the failure of soil around the pile, or structural failure of the pile itself. In order to design a pile foundation safely and economically, accurate assessment of its behavior should be made using pile load tests data and/or the well-known analytical or numerical methods. As the full-scale load tests are very expensive and time consuming, analytical and numerical approaches are usually used to evaluate the lateral behavior of pile-soil systems.

The lateral pile-soil interaction behavior is commonly characterized by a series of uncoupled, nonlinear springs applied along the pile, known as p-y curves. Various formulations have been proposed to predict p-y curves in different site conditions [1-7]. The American Petroleum Institute (API) method [7] is the widely used method based on Matlock's field research [1].

Pile geometry and soil properties are the key parameters in developing p-y curves. These curves mostly depend on the ultimate horizontal soil reaction (P_u) and the critical lateral displacement (y_c) corresponding to 50% mobilized P_u. y_c is defined as:

$$y_c = 2.5\varepsilon_{50}D \tag{1}$$

where, D is the pile diameter, and ε_{50} is the strain at one-half the maximum stress in laboratory undrained compression tests on undisturbed cohesive soil samples. Typical p-y curves for cohesive soils, shown in Figure 1, illustrate the role of the above mentioned parameters on developing such curves. Curves A and B in this figure, are schematic p-y curves for a soil with different ε_{50} values. As $\varepsilon_{50B} > \varepsilon_{50A}$, with the same pile geometry we have $y_{cB} > y_{cA}$. As shown in this figure, ε_{50} is an effective factor in generating p-y curves for clays. It is seen that higher ε_{50} values lead to softer pile behavior and higher lateral displacements for constant lateral load ratios (P/P_u). Furthermore, the ultimate lateral load is obtained at higher levels of pile lateral displacements as ε_{50} increases. Hence, lateral stiffness and resistance of pile-soil system are affected by ε_{50}.

Sullivan et al. [8] recommended ε_{50} values for different clayey soils based on the undrained shear strength. However, such proposed ε_{50} values are not consistent with those obtained from experimental measurements conducted in different sites and do not result in accurate p-y curves in most soil conditions [9-10].

According to [6], the ε_{50} value must be evaluated from the stress-strain curves of soil. Using the hyperbolic curve fitting expression proposed by [11], the following relationship was derived:

$$\varepsilon_{50} = \left(\frac{1}{2 - R_f}\right)\frac{\sigma_f}{E_i} \tag{2}$$

where, R_f= ratio of deviatoric failure stress over deviatoric ultimate stress (take equal to 0.8); σ_f= deviatoric failure stress which is two times of s_u for cohesive soil; s_u= undrained shear strength; and E_i= initial tangent modulus, which, for cohesive soils it is simplified to:

$$\varepsilon_{50} = \frac{1.67 s_u}{E_i} \tag{3}$$

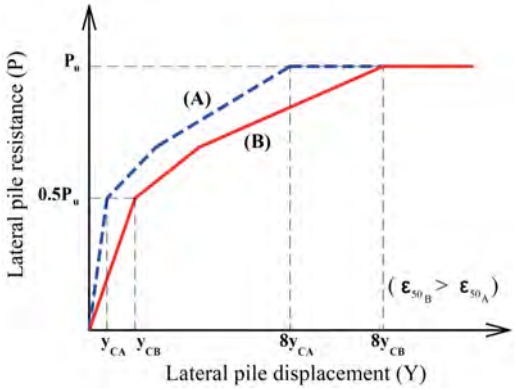

Figure 1: Typical p-y curves for pile in cohesive soil under static loading

Cone penetration test (CPT) is a reliable in-situ test for its continous sounding capability and good repeatability. It provides valuable geotechnical information in soil. Furthermore, the similarity between CPT penetration process and pile installation has led to its popularity in deep foundation analysis and design. Total cone tip resistance obtained from CPT has strong correlation with soil shear strength [12]; on the other hand, due to direct dependence of ε_{50} on shear strength, total tip resistance of CPT can be employed in evaluating ε_{50}.

Despite significant influence of ε_{50} on determining p-y curves, the prediction methods to evaluate this parameter are very rare in the literature. Therefore, this study investigates the use of CPT data to predict ε_{50} in clayey soils and examines the capability of predicted ε_{50} values in generating realistic p-y curves for laterally loaded piles in different sites. The present calculations of ε_{50} are based on a comprehensive databank from laboratory and field tests, performed in South Pars field, Persian Gulf, south west of Iran. The field is an extremely strategic offshore area which contains world's largest gas resources. Many gas extraction facilities supported on long pile foundations have been constructed in this important region and a large number of such facilities is still under development. Hence, this research mainly focuses on accurate evaluation of ε_{50} as an influential parameter in analysis and design of piles against lateral loads in this region. In this regard, several statistical models, based on evolutionary polynomial regression (EPR) method, are proposed to evaluate ε_{50} values for clayey soils. The effects of cone tip resistance, undrained shear strength, overburden pressure as well as different index properties of soils such as overconsolidation ratio and plasticity index on ε_{50} are evaluated and discussed. In particular, the effect of undrained shear strength of cohesive soils obtained from field tests on ε_{50} is investigated and compared with the recommended values available in the literature. Finally, the validation of the proposed models is performed for full scale piles tested in two different sites with different soil conditions.

Site Description

The survey area, approximately 50×45 km^2, is located in Persian Gulf, Iran, between 27° 27' to 27° 28' Northing and 52° 27' to 52° 44' Easting (Figure 2). Soil investigation activities comprised of sixteen boreholes; eight boreholes with 110 m depth and the rest with 80 m depth below the seabed. In-situ and laboratory tests were carried out to determine the geotechnical properties of sub-seabed soils. The in-situ tests included piezocone penetration and torvane. Laboratory tests such as unconsolidated undrained (UU) triaxial compression were performed which resulted in undrained shear strength of soil. The strain at 50% of maximum deviatoric stress (ε_{50}) and strain at failure were also obtained from stress-strain curves in UU tests. Atterberg limits and sieve tests were performed as well. The sub-seabed soils are generally clay, including very soft clay at top up to approximately 20 m which become stiffer with depth. Also lenses of sandy silt and gypsum are found in several depths.

Evolutionary Polynomial Regression

Evolutionary polynomial regression (EPR) is a useful toolbox developed on modeling methodology based on hybrid regression method by [13-14]. It is a symbolic data driven method which is used to create polynomial models to evolutionary compute based on input data and belongs to the Genetic Programming family [15]. The constitutive modeling of soil [16] and assessment of earthquake-induced soil liquefaction and lateral displacement [17] are some successful examples of using EPR in the field of geotechnical engineering.

EPR method includes two general stages; searching the model structures based on an integer Genetic Algorithm (GA) and evaluating each model parameters, such as numeric constant coefficients considering linear optimization [14]. The general symbolic expression derived from EPR is as follows:

$$\hat{Y} = \sum_{j=1}^{m} F(\mathrm{X}, f(\mathrm{X}), a_j) + a_0 \tag{4}$$

Figure 2: Location of survey area in South Pars Field, south-west of Iran

where, $\hat{Y}$ is the estimated outputs of the system derived from EPR; F is the function constructed by the program; X is the input variables matrix; f is a user defined function; a_j is an adjustable parameter determined by the program; and m is the number of terms of the expression defined by user excluding bias a_0, if any.

In order to determine all models corresponding to the optimal trade-off between the fitness and brevity of the model, EPR performs a multi-objective search exhibiting various mathematical models representing best fitness for possible models. For particular purpose, one can choose best models based on short gap reconstruction, gaining physical insight or forecasting the phenomenon. The fitness model defined in EPR is the Coefficient of Determination (*COD*) which refers to how closely the regression expression fits the data points:

$$CoD = 1 - \frac{\sum_{n} (p - m)^2}{\sum_{n} (m - \overline{m})^2} \tag{5}$$

where, P is the predicted values by model derived from EPR; m is the measured values; $\overline{m}$ is the average of measured values; and n is the number of data points. More details about EPR architecture for model representation as well as the method employed for parameter estimation can be found in [14].

Results and Discussion

The field and laboratory test results including 274 data series are considered as the databank for the numerical regression. In the present study, five variables are identified as primary input data of cohesive soils for evaluating ε_{50} as an output. The input data includes undrained shear strength (s_u), normalized cone tip resistance (q_c), total overburden pressure (σ_0), plasticity index (*PI*) and overconsolidation ratio (*OCR*).

In pattern recognition procedures, it is common practice to divide the available data into two subsets; training and testing. The model is firstly developed using the former and then tested using the latter one to ensure that the final obtained model has the ability to properly estimate ε_{50} for unseen or untrained cases. Here, the entire databank is divided into several random combinations of training and testing sets until a robust representation of the whole population, in terms of statistical properties, is achieved for both training and testing sets. The statistical properties of the parameters considered in this study including the values of maximum, minimum, mean, and standard deviation are presented in Table 1 for training, testing and all datasets. Training dataset includes 80% of all data (219) and the rest

(55) are used as testing dataset. The statistical values of training, testing and all dataset, shown in Table 1, are close to each other.

After several analyses in EPR framework, four relationships are developed for evaluating ε_{50}, which are presented in Table 2. To examine the robustness and assess the performance of EPR models, the following three statistical criteria have been used:

- Coefficient of determination (R^2), is a measure used to determine the relative correlation between two sets of variables, and defined as:

$$R^2 = 1 - \frac{\sum_{i=1}^{n}(m_i - p_i)^2}{\sum_{i=1}^{n}(m_i - \overline{m})^2} \tag{6}$$

- Root mean square error (*RMSE*), is a measure of error, defined as:

$$RMSE = \sqrt{\frac{\sum_{i=1}^{n}(m_i - p_i)^2}{n}} \tag{7}$$

The advantage of this criterion is that large errors receive greater attention than smaller ones.

- Mean absolute error (*MAE*), is another measure of error which eliminates the emphasis given to large errors, presented as:

$$MAE = \frac{\sum_{i=1}^{n}|m_i - p_i|}{n} \tag{8}$$

In the above relations, m_i and p_i are the i^{th} measured and predicted values of output parameter (ε_{50}), respectively; n is the number of data points; and $\overline{m}$ indicates the average of measured output.

Table 1: Statistical characteristics of databank

Subsets	Statistic al characteristics	σ_0 (*kPa*)	s_u (*kPa*)	q_c (*kPa*)	*PI* (%)	*OCR*	Measured ε_{50} (%)
Testing data (55 data)	Minimum	216	19	162	14	0.9	0.9
	Minimum	1933	504	8767	40	4	9.2
	Mean	1081	241	4155	29	2.2	3.9
	Standard deviation	462	112	2190	6.8	0.74	2.1
Training data (219 data)	Minimum	217	19	139	12	0.9	0.7
	Minimum	2207	634	8943	47	5.3	9.3
	Mean	1077	274	4184	30	2.4	3.5
	Standard deviation	515	129	1996	7.4	1.1	2.0
All data (274 data)	Minimum	216	19	139	12	0.9	0.7
	Minimum	2207	634	8943	47	5.3	9.3
	Mean	1078	268	4178	30	2.4	3.6
	Standard deviation	505	126	2037	7.3	1.0	2.1

The suggested models to evaluate ε_{50} as well as the values of statistical criteria are presented in Table 2. It is seen that the performance of models improves from Model 1 to 4 since R^2 value increases while *RMSE* and *MAE* values decrease. Based on the results summarized in Table 2, the EPR Model 4 is chosen as the most appropriate one which is developed using four input parameters: q_c, σ_0 , *PI*, *OCR*.

The first relationship is developed between undrained shear strength of soil and ε_{50} and the second one uses the normalized cone tip resistance (q_c) to predict ε_{50}, as shown in Table 2. By comparing the statistical characteristics of Models 1 and 2, it can be found that the ε_{50} values predicted from field-based resistance property (q_c) are more accurate than those predicted from the laboratory-based resistance (s_u). By using q_c instead of s_u, R^2 increases from 6.6 for Model 1 to 20.8 for Model 2. However, R^2 value is not yet acceptable enough, and it seems that other influential parameters should be included in the model development process. Therefore, after several try and error procedures, it was found that the index properties of soil, e. g., *OCR* and *PI* have strong effects on the predicted ε_{50} values. According to Table 1,

it is realized that Model 3, which includes the above mentioned factors, predicts ε_{50} more accurately than Model 2. Furthermore, Model 4 shows that the overburden pressure has also a notable positive influence on prediction accuracy.

Table 2: Proposed models for estimating ε_{50}

No. of Model	Equation	Involved parameters	R^2 (%)	*RMSE*	*MAE*
Model 1	$\varepsilon_{50} = -0.79 + 1.5 s_u^{\,0.2}$	s_u	6.6	1.99	1.65
Model 2	$\varepsilon_{50} = 1.48 + 1.2\times10^{-3} q_c^{\,0.9}$	q_c	20.8	1.84	1.52
Model 3	$\varepsilon_{50} = 4.84 - 8.76\times10^{-2} q_c^{\,0.3} PI^{\,0.5} OCR^{-0.1} - 1.24\times10^{-12} q_c^{\,3.3} OCR^{-0.3} + 5.43\times10^{-6} q_c^{\,1.4} PI^{\,0.7} OCR^{-0.1} - 2.1\times10^{-3} q_c^{\,0.5} PI^{\,0.8} OCR^{0.7}$	q_c, *PI*, *OCR*	36.7	1.64	1.34
Model 4	$\varepsilon_{50} = -2.7\times10^{-13} \sigma^{1.5} q_c^{\,2.6} PI^{\,-1.3} OCR^{-0.2} - 1.8\times10^{-10} \sigma^{0.6} q_c^{\,1.3} PI^{\,1.6} OCR^{2} + 1.5\times10^{-6} \sigma^{1.5} q_c^{\,0.4} PI^{\,0.1} OCR^{0.6} + 1.55$	σ_0, q_c, *PI*, *OCR*	64.8	1.22	1.02

Figure 3 illustrates the predicting capability of models by plotting the predicted ε_{50} (ε_{50p}) values against their corresponding measured values (ε_{50m}) in training and testing datasets and their statistical characteristics are shown for quantitative comparison. Considering the data scatter in the graphs of Figure 3, the results of models for testing dataset are generally consistent with those for training dataset. The more the points are distributed uniformly around the ideal 45° line, and the less scattering around this line, the better the capability of the model in predicting ε_{50}. In this regard, it is clear that Model 4 behaves better than the other ones. The upper and lower lines in Figure 3 show the boundaries for a zone that is characterized by the ratios of predicted to measured ε_{50} between 0.5 and 2.0. The estimation quality (*EQ*) of each model, defined as the number of the points that fall inside these two boundaries as percent of the total points is shown in the figure. As the performance of models improves, the data show more concentration in the mentioned zone. While all models show acceptable estimation qualities, the estimation quality for Model 4 has the highest value of 91.6% among the proposed models.

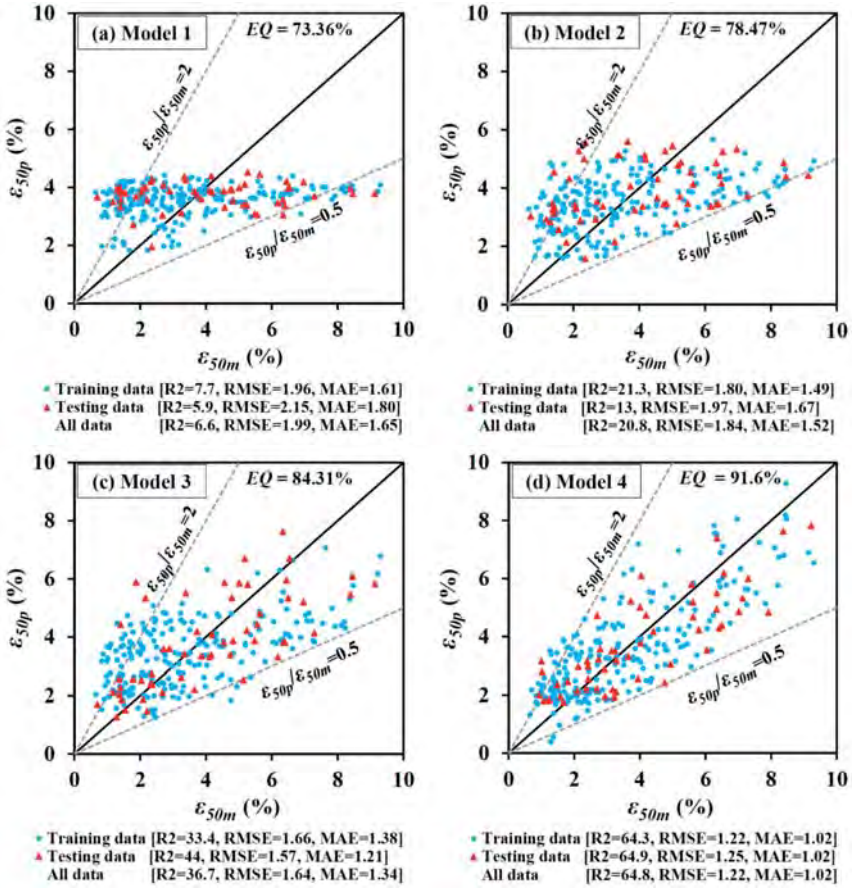

Figure 3: Predicted versus measured ε_{50} values for proposed EPR-based models

It is seen in Figure 3 that the predicted ε_{50} values from Model 1, which was developed merely from undrained shear strength (s_u), are not well-distributed along the diagonal line and are concentrated in a narrow horizontal band.

However, implementing the normalized cone tip resistance (q_c), instead of s_u, in Model 2 has smoothed the above mentioned shortcoming.
The log normal distribution, used by [18], is an appropriate statistical criterion to further evaluate the performance of the proposed models. In this regard, the natural logarithm of the ratio of predicted to measured ε_{50}, ($\ln(\varepsilon_{50p}/\varepsilon_{50m})$), is calculated for each data point and then the mean and standard deviation of these values are determined as follows:

$$\mu_{\ln(\varepsilon_{50p}/\varepsilon_{50m})} = \frac{1}{n}\sum_{i=1}^{n} \ln(\varepsilon_{50p}/\varepsilon_{50m})_i \tag{9}$$

$$\sigma_{\ln(\varepsilon_{50p}/\varepsilon_{50m})} = \sqrt{\frac{1}{n-1}\sum_{i=1}^{n}\left(\ln(\varepsilon_{50p}/\varepsilon_{50m})_i - \mu_{\ln(\varepsilon_{50p}/\varepsilon_{50m})}\right)^2} \tag{10}$$

where, the subscripts p and m denote "predicted" and "measured", respectively; n is the number of data considered in the analysis; $\mu_{\ln}$ and $\sigma_{\ln}$ are indicators for accuracy and precision of the models, respectively, which are used to identify the log normal distribution of the density function as:

$$f(\varepsilon_{50p}/\varepsilon_{50m}) = \frac{1}{\sqrt{2\pi}\sigma_{\ln}(\varepsilon_{50p}/\varepsilon_{50m})}\exp\left[-\frac{1}{2}\left(\frac{\ln(\varepsilon_{50p}/\varepsilon_{50m}) - \mu_{\ln(\varepsilon_{50p}/\varepsilon_{50m})}}{\sigma_{\ln(\varepsilon_{50p}/\varepsilon_{50m})}}\right)^2\right] \tag{11}$$

The better distribution is achieved when $\mu_{\ln(\varepsilon 50p/\varepsilon 50m)}$ and $\sigma_{\ln(\varepsilon 50p/\varepsilon 50m)}$ approach unity and zero, respectively.
The probability of predicting ε_{50} with 0 to 90% accuracy (10-100% absolute error) is calculated from log normal distributions of $\varepsilon_{50p}/\varepsilon_{50m}$ and shown in Figure 4. At a specified absolute error level, the probability of predicting ε_{50} is derived by calculating the total area below the log normal distribution curve within the accuracy limits. At a constant absolute error, a higher probability indicates the better ability of model in predicting ε_{50}. Based on this definition, the performance of the models improves from Model 1 to 4 at all levels of absolute error.

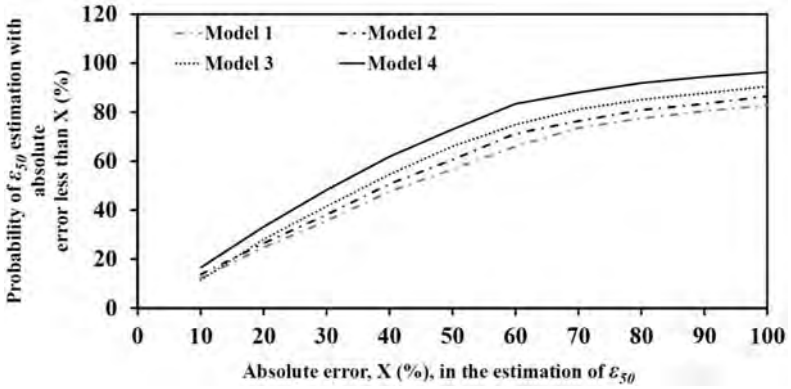

Figure 4: Probability of ε_{50} estimation with absolute error less than a given error, x (%)

The ability of different models to predict ε_{50} can be evaluated using cumulative probability (*CP*), as used by [19]. They used the concept of cumulative probability as a criterion to evaluate the bias of their model. The cumulative probability for each $\varepsilon_{50p}/\varepsilon_{50m}$ can be obtained by the following definition:

$$CP_i = \frac{i}{n+1} \tag{12}$$

where, i is the data number, arranged in an ascending order. The cumulative probability versus the ratio $\varepsilon_{50p}/\varepsilon_{50m}$ for the proposed models is depicted in Figure 5. In order to assess the ability of each model in estimating ε_{50}, the 50% and 90% cumulative probabilities (CP50% and CP90%) are calculated. The difference between CP90 and CP50 (CP90%-CP50%) represents the discrepancy from accurate estimation. Ideally, if all data are predicted with no bias, the distribution of estimated to measured ε_{50} against CP will be a straight line with value of unity, indicating an exact estimation. In reality, the better performance of the model is achieved when $\varepsilon_{50p}/\varepsilon_{50m}$ is closer to unity at CP50%. Lower (CP90%-CP50%) for each model indicates the better prediction accuracy of the proposed model. According to this criterion, it is observed in Figure 5 that Model 4 leads to the optimum value of CP50% equal to unity and lower value of (CP90%- CP50%) compared with the other models.

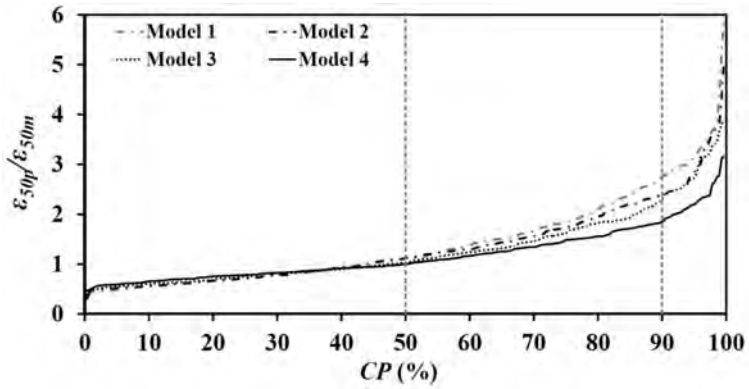

Figure 5: Cumulative probability plot of $\varepsilon_{50p}/\varepsilon_{50m}$ for proposed models

In statistical analysis, a model would behave better, if residual values, i.e. the difference between the measured and predicted values of ε_{50}, are concentrated more uniformly around the mean value of residuals. The mean value of residuals is calculated by:

$$MR = \frac{1}{n}\sum_{i=1}^{n}(\varepsilon_{50m} - \varepsilon_{50p})_i \tag{13}$$

Figure 6 depicts the residuals of the training and testing sets for all presented models versus data number. In this figure, the residuals are scattered along a line indicating the mean (*MR*). In addition, the upper and lower bounds of residual scattering (*MR*±*σ*; *σ* is standard deviation of residuals) are shown in the figure. The ideal performance of each model is achieved by *MR* and *σ* equal to zero. In general, the lower absolute values of these two parameters represent the better performance of the model. A comparison between the proposed models in Figure 6, with respect to the above parameters, shows the improvement of the Models from 1 to 4 by decreasing absolute *MR* and *σ* values.

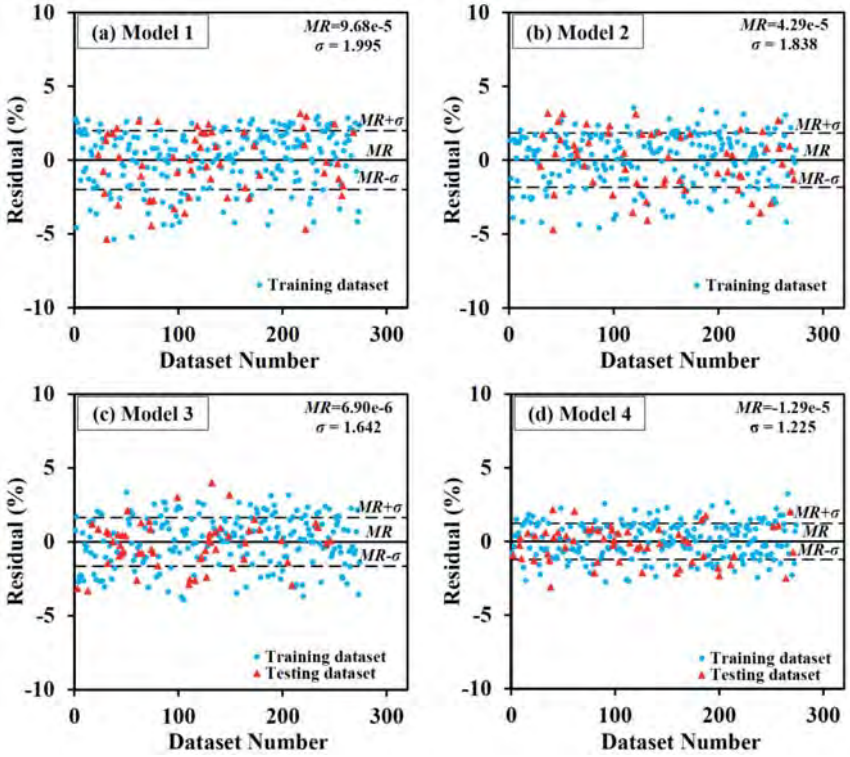

Figure 6: Distribution of residuals for EPR-based models

Validation of Proposed Models

Field verification

In order to validate the proposed models, the test results in three boreholes of a site are considered. The site is located at South Pars field, Persian Gulf, Iran, outside the survey area, shown as site 1 in Figure 2. The soil is very soft clay overlying a sandy silt or silty sand layer at shallow depths. Stiff to very stiff clay dominates at deeper parts. The profile of soil properties in 3 boreholes within this site are presented in Figure 7. Figure 8 shows ε_{50} values predicted by different models as well as the measured values obtained from UU tests in borehole depths. In all figures, the recommended ε_{50} values by Sullivan et al. [8] are significantly lower than the measured ones. However, ε_{50} values

predicted by Models 1 and 4 compare relatively well with the measured ones in the full range of values along borehole depths, as shown in Figure 8. Generally, ε_{50} values show an increasing trend with depth from both laboratory measurements and the currently proposed models predictions. This result is in contradiction with the values of ε_{50} recommended by Sullivan.

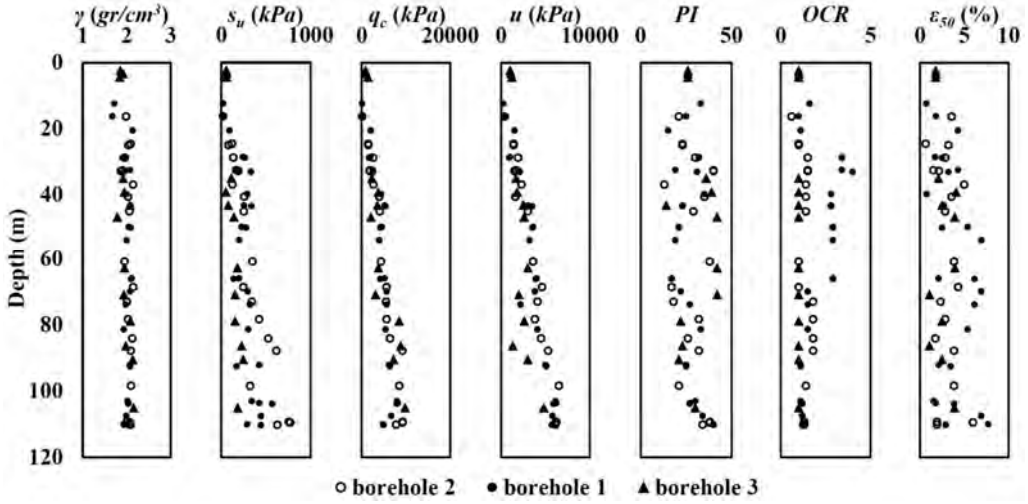

Figure 7: Geotechnical characteristics of soil in the boreholes of site 1

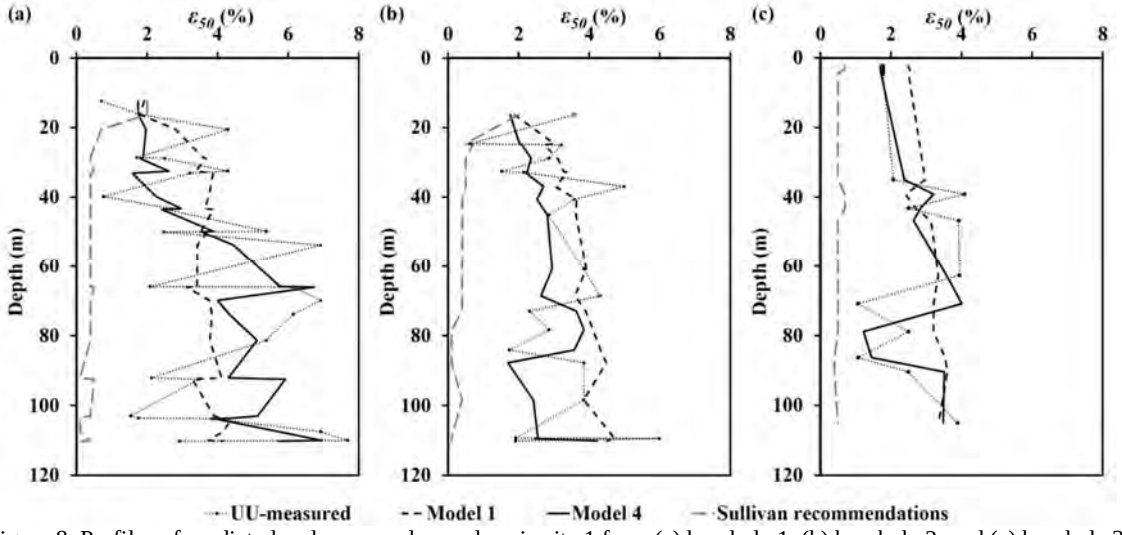

Figure 8: Profiles of predicted and measured ε_{50} values in site 1 from (a) borehole 1, (b) borehole 2, and (c) borehole 3

Numerical Simulation

In order to show the efficiency of best proposed model (Model 4) in predicting the lateral response of pile-soil systems, a numerical study was considered. In this regard, the lateral response of a given pile-soil system with about 100m length, 152.4cm diameter, was modeled using finite element while the value of ε_{50} included in this model was firstly substituted by measured ε_{50} values and then by those predicted from Model 4. For better comparison of the performance of the proposed model in predicting the lateral pile-soil response, similar simulations were also performed by ε_{50} recommendations of Sullivan et al., [8] and those from Robertson et al., [6] and the obtained results were compared.

The soil profile modeled in the numerical study is generally consists of clayey soil with undrained shear strength ranged from 70-650 *kPa*, effective unit weight of 5.8-12.6 kN/m^3 and ε_{50} ranged from 0.05-8.5.

The numerically modeled pile-soil was laterally loaded and its lateral response containing lateral displacement, moment and shear were compared through various methods of ε_{50} estimation. The variations of lateral response of pile-soil along depth corresponding to various methods are depicted in Figure 9. The lateral responses of pile-soil system using measured ε_{50} values are also shown in this figure. As can be seen, lateral response of pile-soil is considerable only in the upper 40 m soil below the mudline and after that the pile is thoroughly fixed into the soil. It is in accordance to previous results reported in the literature that the most of lateral capacities and deformations of the piles are dependent to the characteristics of the upper part of soil, depending on their diameters [20-21]. However, it is clearly observed that the lateral response of pile in upper portion of the soil is dependent to what value of ε_{50} included in the numerical simulation. Compared to the three response curves obtained from measured ε_{50}, the curve corresponding to Model 4 of this study is of the best performance. Figure 9 shows that the use of Sullivan et al., [8] recommendations resulted unconservative displacements while the use of Robertson et al., [6] model introduce conservative to the obtained results.

The results of the numerical study also proved the preference of proposed model to other available recommendations in the literature about the prediction of ε_{50}.

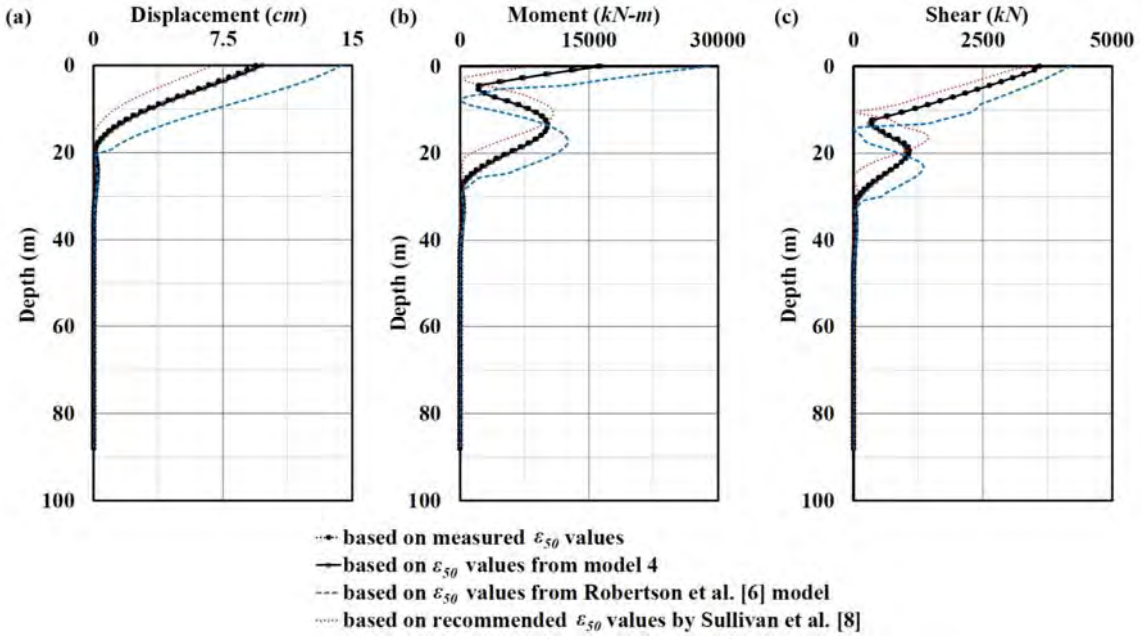

Figure 9: Numerical analysis results of lateral response of typical pile-soil system

Summary and Conclusions

In this research, the results of field and laboratory tests data in South Pars field, Persian Gulf, Iran, are used to develop models for evaluating ε_{50} using EPR. In this regard, cone tip resistance of CPT and several parameters of cohesive soils (s_u, σ_0, *OCR* and *PI*) are considered in developing models. The conclusions are drawn as follows:

- According to the statistical analyses, the models developed using cone tip resistance (q_c) yield more accurate ε_{50} values than those developed using undrained shear strength of soils (s_u) obtained from UU tests. In general, ε_{50} is more realistically predicted using field-based, instead of laboratory-based, resistance of soil.
- The index properties of soil, e.g. *OCR* and *PI*, significantly improve the performance of the proposed models in predicting ε_{50}.
- According to statistical criteria, the models which are developed considering the effect of overburden pressure (σ_0) lead to better predicted ε_{50} values.
- The models are validated with the field data of a site, located outside the survey area. The predicted ε_{50} values are in relatively well agreement with the measured ones in the full range of values along all boreholes depths in this site. It is found that the predicted ε_{50} values from the proposed models increase with soil depth which agrees with the laboratory measurements.
- A numerical simulation shows that while the use of Sullivan et al. [8] recommendations resulted unconservative displacements and the use of Robertson et al. [6] model introduce conservativeness to the obtained results, the proposed model can interestingly used to obtain accurate results.

Acknowledgment

The authors would like to thank Mrs. Omrani for her effective cooperation in numerical modeling of the lateral pile responses, presented in this study.

References

[1] Matlock, H., "Correlations for design of laterally loaded piles in soft clay," Proceeding of Offshore Technology Conference, H. M. Coyle and R.E. Bartoskewitz, eds., Houston, Texas, pp. 577-594, 1970.

[2] Reese, L. C., and Welch, R. C. "Lateral loading of deep foundations in stiff clay," Journal of Geotechnical and Geoenvironmental Engineering, 101(7):633-49, 1975.

[3] Reese, L. C., Cox, W. R., and Koop, F. D., "Field testing and analysis of laterally loaded piles in stiff clay," Proceeding of Offshore Technology Conference, Houston, Texas, 2312. pp. 671-690, 1975.

[4] O'Neill, M. W., Gazioglu, S. M., "Evaluation of p–y relationships in cohesive soils," Proceeding of Symposium Analysis and Design of Pile Foundations, ASCE, 1-5 October, pp. 192–213, 1984.

[5] Gabr, M. A., and Borden, R., "Analysis of load deflection response of laterally loaded piers using DMT," Proceeding of 1st International Symposium on Penetration Testing, Balkema, Rotterdam, The Netherlands, pp. 513-520, 1988.

[6] Robertson, P. K., Davies, M. P., and Campanella, R. G., "Design of laterally loaded driven piles using the flat dilatometer," Geotechnical Testing Journal, 12(1), pp. 30-38, 1989.

[7] American Petroleum Institute, "Recommended practice for planning, designing and constructing fixed offshore platforms," API recommended practice RP-2A, Washington, D.C., 1993.
[8] Sullivan, W. R., Reese, L. C., and Fenske, C. W., "Unified method for analysis of laterally loaded piles in clay," Numerical Methods in Offshore Piling. ICE, London, pp. 135-146, 1980.
[9] Hamilton, J. M., and Dunnavant, T. W., "Analysis of behavior of the Tilbrook Grange lateral test pile" Large-scale pile tests in clay. Edited by J. Clarke, Thomas Telford, London, U.K. pp. 448-461, 1993.
[10] Hamilton, J. M., Long, M. M., Clarck J., and Lambson M. D., "Cyclic lateral loading of an instrumented pile in overconsolidated clay at Tilbrook Grange," Large-scale pile tests in clay. Edited by J. Clarke, Thomas Telford, London, U.K. pp. 381-403, 1993.
[11] Konder, R. L., Zelasko, J. J., "A hyperbolic stress-strain formulation in sands," Proceeding of 11th Pan American Conference on Soil Mechanics and Geotechnical Engineering 1, pp. 289-324, 1963.
[12] Lunne, T., Robertson, P. K., and Powell, J. J. M., "Cone penetration testing in geotechnical practice," Blackie Academic, EF Spon/Routledge Publication, New York, 1997.
[13] Giustolisi, O., Savic, D. A., and Doglioni, A., "Data reconstruction and forecasting by evolutionary polynomial regression," Proceeding of 6th International Conference of Hydroinformatics, Singapore, **2**, pp. 1245-1252, 2004. ISBN 981-238-787-0.
[14] Giustolisi, O., and Savic, D. A., "A symbolic data-driven technique based on evolutionary polynomial regression," Journal of Hydroinformarics, 8(3), pp. 207-222, 2006.
[15] Koza, J. R., "Genetic Programming: On the Programming of Computers by Natural Selection," MIT Press, Cambridge, MA. ISBN 0-262-11170-5, 1992.
[16] Javadi, A. A., and Rezania, M., "Intelligent finite element method: An evolutionary approach to constitutive modeling," Advanced Engineering Informatics, 23, pp. 442-451, 2009.
[17] Rezania, M., Faramarzi, A., and Javadi. A. A., "An evolutionary based approach for assessment of earthquake-induced soil liquefaction and lateral displacement," Engineering Applications of Artificial Intelligence, 24, pp. 142-153, 2011.
[18] Briaud, J. L., and Tucker, L. M., "Measured and predicted axial response of 98 piles," Journal of Geotechnical Engineering, 114(9), pp. 984-1001, 1988.
[19] Long, J. H., and Wysockey, M. H., "Accuracy of methods for predicting axial capacity of deep foundations," Proceeding of OTRC' 99 Conference, Analysis, Design, Construction, and Testing of Deep Foundation, ASCE, Geotechnical Special Publication 88, pp.190-195, 1999.
[20] Briaud, J. L., "SALLOP: simple approach for lateral loads on piles," Journal of Geotechnical and Geoenvironmental Engineering ASCE, 123(10), pp. 958-964, 1997.
[21] Chen, J. Y., Matarek, B. A., Carpenter, J. F., and Gilbert, R. B., "Analysis of Potential Conservatism in Foundation Design for Offshore Platform Assessment," Final Project Report Prepared for the American Petroleum Institute Under Contract, No. 2007-103130, 280 pp, 2010.